C. MONACO(*) & G. VENTURA(**)

MAGMATIC AND STRUCTURAL FEATURES OF THE "VALVERDE CENTER" (MT. ETNA, SICILY)(***)

CONTENTS

ABSTRACT

On the southeastern slope of M.te Etna (Sicily) a small-sized eruptive center ("Valverde Center") has been identified. It formed during the early stage of activity of M.te Etna (150-100 Kyr).

Stratigraphical and volcanological data allow to distinguish three main eruptive cycles of the "Valverde Center". Cycle I is characterized by the emission of lava flows of basaltic to hawaiitic composition. The products of Cycle II show compositions similar to Cycle I and are related to phreatomagmatic, effusive and strombolian activities. The products of Cycle III (pumice fall and flow deposits) show evolved compositions (high-SiO_2 benmoreites and trachites). The petrochemical characters of the erupted products are the result of crystallization and mixing of melts generated from a heterogeneous source.

The Valverde center is affected by a NNE-SSW to NNW-SSE trending fault system, active since Middle Pleistocene. These structures, related to a WNW-ESE extension, consist of east-dipping normal faults with a right lateral component of motion (oblique extension) along the NNW direction. The geometry of the fault system is consistent with classical oblique rifting models. The progressive development of fracture zones along the main fault segments favoured the formation of magmatic reservoirs in which magmas may easily mix and crystallize. This agrees with experimental studies on wrench fault tectonics.

RIASSUNTO

Sul basso versante sud-orientale del Monte Etna (Sicilia) è stato identificato un piccolo centro eruttivo ("Centro di Valverde") formatosi durante i primi stadi dell'evoluzione dell'apparato etneo (150.000-100.000 anni).

Dati stratigrafici e vulcanologici permettono di distinguere tre principali cicli eruttivi del "Centro di Valverde". Il Ciclo I è caratterizzato dall'emissione di colate laviche a composizione hawaitica. I prodotti del Ciclo II mostrano composizioni simili a quelli del Ciclo I e sono correlati ad attività freatomagmatica, effusiva e stromboliana. I prodotti del Ciclo III (depositi di caduta e di flusso) mostrano composizioni evolute (benmoreiti ad alto contenuto in SiO_2 e trachiti). I caratteri petrochimici dei prodotti eruttati sono il risultato della differenziazione di fusi generati da una sorgente eterogenea.

Il Centro di Valverde è dislocato da un sistema di faglie orientate da NNE-SSW a NNW-SSE, attivo a partire dal Pleistocene medio. Queste strutture, correlate a un'estensione regionale orientata WNW-ESE, consistono in una serie di faglie normali immergenti verso est e mostranti una componente di movimento destro lungo la direzione NNW.

La geometria del sistema di faglie, legata a estensione obliqua, è in accordo con i modelli classici sul *rifting* obliquo. Il progressivo sviluppo di zone di frattura lungo i principali segmenti di faglia ha favorito la formazione di "*reservoir*" in cui il magma ha potuto differenziarsi. Questo è in accordo con gli studi sperimentali sulla tettonica trascorrente.

KEY WORDS: Volcanism, Extension, Mt. Etna.

PAROLE CHIAVE: Vulcanismo, Estensione, M. Etna.

INTRODUCTION

Mt. Etna (Eastern Sicily; Fig. 1) is a Quaternary composite volcano characterized by Na-alkaline magmatism (CRISTOFOLINI & ROMANO, 1982; CHESTER *et alii*, 1985). It has developed within a rifted area located on the external front of the Maghrebian Chain (Fig. 1). The volcanic edifice, overlying Middle Pleistocene sediments and volcanics (pre-Etnean volcanism), is made up of several sequences related to different eruptive centers. The sequences have been grouped into three main volcano-stratigraphic units, known as Ancient Alkali Centers (AAC), Trifoglietto Unit and Mongibello Unit (ROMANO, 1982; CRISTOFOLINI *et alii*, 1991), separated by major unconformities linked to volcano-tectonic collapses.

The aim of this study is to investigate the relationships between tectonic structures and volcanism in a small-sized eruptive center, previously undescribed in the literature, located on the south-eastern slope of Mt. Etna. This volcanic edifice, here called the "Valverde center", belongs to the AAC. This study, based on field mapping (scale 1:10.000) and stratigraphic analysis, has been supported by morphotectonic observations and by petrographical and geochemical analyses of the erupted products. The Valverde Center, whose products are basalts-hawaiites and trachytes (without intermediate compositions), is characterized by oblique-extension. Recent studies on volcanism occurring in areas characterized by oblique rifting processes (i.e. Strait of Sicily (Pantelleria), CELLO *et alii*, 1985; Mean Ethiopian Rift, BOCCALETTI *et alii*, 1992; Lipari Island, Southern Tyrrhenian Sea, CRISCI *et alii*, 1991; Oligo-Miocene magmatism in Yemen,

(*)Istituto di Geologia e Geofisica - Università di Catania.
(**)Dipartimento di Scienze della Terra - Università della Calabria - Cosenza. Present address: Osservatorio Vesuviano, Ercolano (NA).

(***)Study financially supported by M.U.R.S.T. and C.N.R. (grant n. 9400184.05).

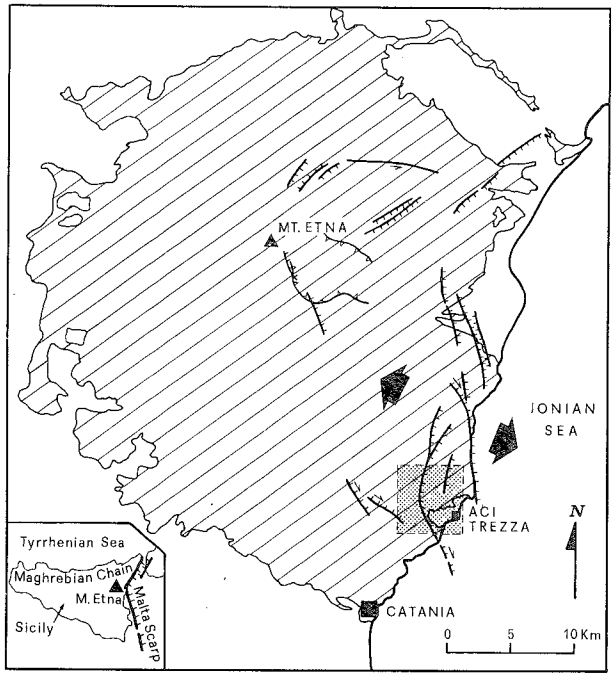

Fig. 1 - Structural sketch map of Mt. Etna and location of the studied area (dotted square). Lines indicate the main faults (barbs on the hanging-wall), black arrows show the direction of extension. From Lo Giudice *et alii* (1982), modified.

Civetta *et alii*, 1992) similarly indicate a bimodal distribution in the composition of the erupted products. This feature is well recognizable in large volcanic provinces (i.e. Yemen) as well as in composite volcanoes (Lipari Island). The recognized strong tectonic control on the magmatic evolution of the Valverde Center allows to analyse in detail the influence of oblique-extension processes on the evolution of the volcanism.

GEOLOGICAL FRAMEWORK

The studied area is located on the south-eastern slope of Mt. Etna (Fig. 1). In this area, the pre-Etnean volcanism is represented by the occurrence of 200 to 500 Kyr old submarine volcanics showing tholeiitic affinity (Romano, 1982; Condomines *et alii*, 1982; Chester *et alii*, 1985). The early occurrence of this volcanism was coeval to the sedimentation of the Middle Pleistocene marly clay sequence outcropping south of Mt. Etna and along the Ionian coast (Wezel, 1967; Kieffer, 1985). The pre-Etnean volcanic products outcrop between Ficarazzi and Aci Trezza, above or within the marly clays (Fig. 2).

The Valverde volcanic products, which belong to the AAC for the stratigraphic position, petrographic features and geochemistry (Romano & Sturiale, 1981; Kieffer, 1985), overlie the pre-Etnean volcanics and sediments. The AAC were active since 150-160 Kyr (Condomines & Tanguy, 1976; Condomines *et alii*, 1982), when changes in the magma feeding system and ascent mechanisms occurred (Tanguy, 1978; Cristofolini & Romano, 1982). This involved a change in the composition of the erupted products (from tholeiitiitic to Na-alkaline volcanics) and in character of volcanism (from fissural to central activity). According to Kieffer (1985) and Kieffer & Tanguy (1993), from 150 to 100 Kyr strombolian and effusive activity mainly occurred with the building up of a large strato-volcano consisting of several eruptive centres; from 100 to 70 Kyr, more explosive activity gave rise to strong phreatomagmatic eruptions which partially destroyed the former eruptive centres. The further dismantling of the AAC cones could have been caused by volcano-tectonic collapses due to the emptying of the shallow feeding fissures following intense explosive and/or effusive activity (Romano, 1982).

The area investigated in this study is affected by a NNE-SSW to NNW-SSE trending normal fault system (Fig. 1). This consists of several east-dipping fault segments active since Middle Pleistocene, characterized by a slightly right-lateral component of motion along the NNW-SSE directions (Lo Giudice *et alii*, 1982). These structures, related to a WNW-ESE regional extension (Bousquet *et alii*, 1987; Monaco & Tortorici, 1995), may represent the northernmost branches of the Malta fault escarpment (Lo Giudice *et alii*, 1982).

MORPHOTECTONICS

North-west of Aci Trezza (Fig. 2), there is good morphological evidence to support the presence of an old dissected volcanic center (Valverde Center), partially covered by more recent products. This interpretation is suggested by a subelliptical (horse-shoe) feature occurring around the Nizzeti area (Fig. 2). This is a northwards open depression, surrounded along the other sides by up to 100 m high scarps made up of volcanic strata showing dips consistent with a cone-shaped morphology. On the western scarp (Valverde-Mt. d'Oro high), lava flows dip counterslope (to the west) with respect to the present Mt. Etna edifice (Figs. 1 and 2). The west-dipping lava flows have been previously considered as the result of tectonic tilting related to N-S trending fault-system activity (Romano & Sturiale, 1981; Kieffer, 1985). However we consider that the Valverde-Mt. d'Oro high represents the remnant of the western slope of the Valverde Center, and that there is no need to invoke tectonic tilting. The south-eastern sector of the volcanic center is recognized by the occurrence of remnants of an arc-shaped scarp, flanking the Nizzeti depression (Fig. 2). The eastern sector is represented by the Torre Casalotto ridge, made up of east-dipping volcanics, which culminates at 219 m a.s.l. (Fig. 2).

Faulting activity, erosion and recent lava cover make it difficult to reconstruct the originary morphology of the Valverde center. East of Valverde (Fig. 2), the volcanic edifice is downthrown seawards by several N5-20°E trending normal faults, splaying out from the northern tip of the NW-SE trending master fault (Nizzeti fault system). The westernmost segments of the Nizzeti fault system give rise to a high scarp, up to 100 m, extending north of Aci San Filippo and showing a right-stepping en-echelon arrangement with respect to the "Timpa di Acireale" fault scarp (Lo Giudice *et alii*, 1982; Monaco *et alii*, 1995). The latter, with a height of 100-120 m, defines the coastline to the north-east (Fig. 1). The Nizzeti fault system is partially covered by recent lava flows which have been in turn downfaulted (Fig. 2) with offsets up to 5 m.

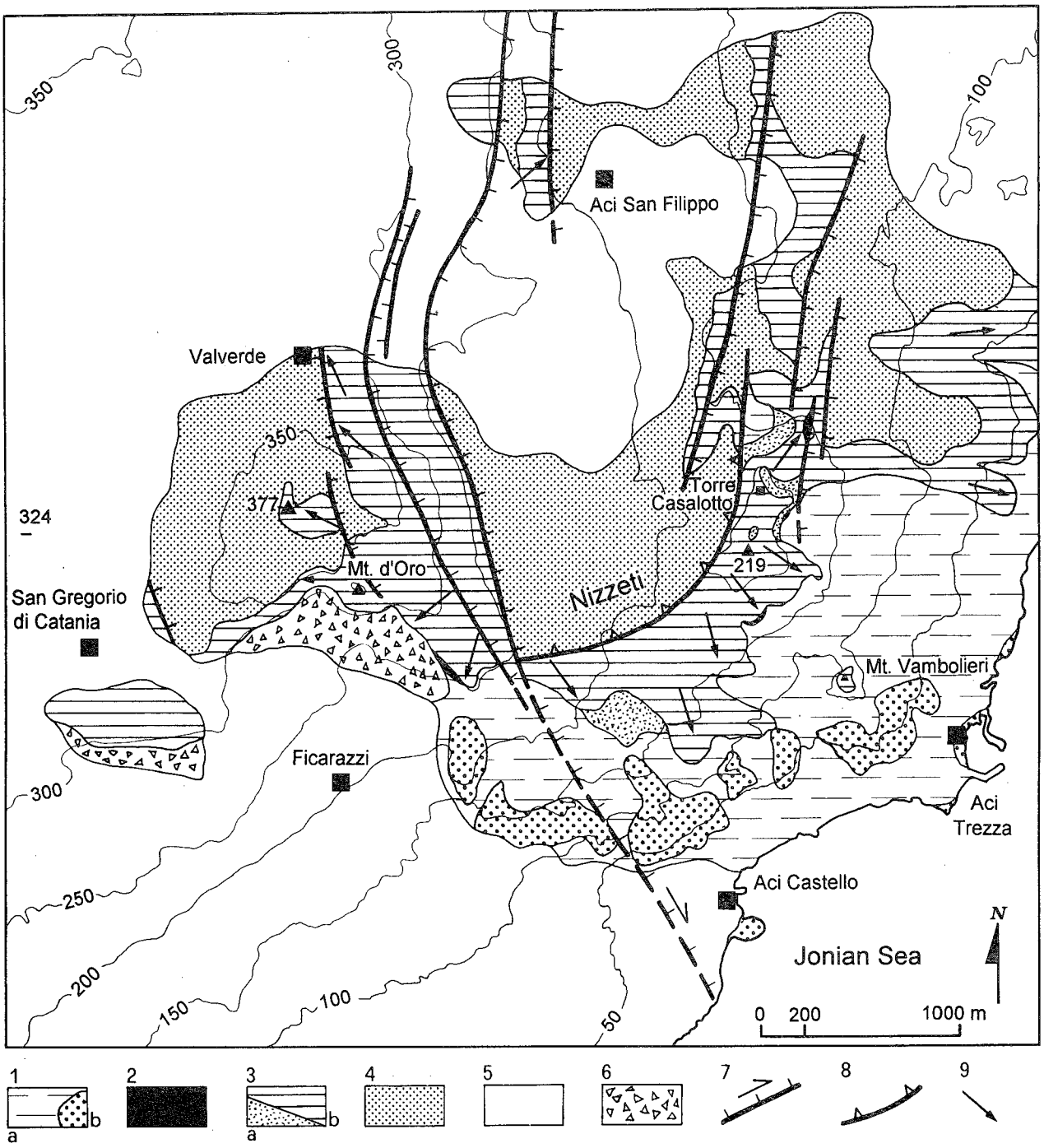

Fig. 2 - Geological sketch map of the Valverde center. Key: 1a, Marly clays (Middle Pleistocene); 1b, pre-Etnean volcanics with tholeiitic affinity (Middle Pleistocene); 2, Cycle I lavas; 3a, Cycle II ash-flow deposits; 3b, Cycle II lavas and strombolian fall deposits; 4, Cycle III pyroclastics; 5, Recent lava flows related to the Mt. Etna activity; 6, debris deposits; 7, fault (dashed where inferred, barbs on hanging-wall); 8, volcano-tectonic collapse scarp; 9, lava flow direction.

The Nizzeti fault system has been seismically active in historical times. Two earthquakes of low intensity (MKS = V and VII) occurred in the 19th century (Imbò, 1935). Moreover aseismic creep (Lo Giudice & Rasà, 1986), with oblique motion (dextral), occurs along the fault north of Aci San Filippo where ground fractures and damage to buildings have been observed.

The overall geometry of the Nizzeti fault system, together with data from the literature (Lo Giudice *et alii*, 1982), and field observations, suggests a right lateral component of motion for the NW-SE trending fault segments even if it is very difficult to estimate the amount of the horizontal component.

Slope failure has further contributed to the partial collapse of the Valverde edifice. South of Mt. d'Oro, is a palaeo-landslide (Fig. 2), probably placed in correspondence of an E-W oriented ancient coastline, whereas more recent landslides have occurred in the M. Vambolieri area.

Faulting activity has also been accompanied by a strong uplift of the whole area since the Middle Pleistocene (Kieffer, 1971; Monaco *et alii*, 1995). The

uplift (0.7-1.7 mm/yr) is testified by old shorelines, marked by beach deposits, located at 220 m a.s.l. (Ficarazzi), 130 m a.s.l. (M. Vambolieri), 60 m, 35 m and from 16 to 1 m a.s.l. (between Aci Castello and Aci Trezza) (KIEFFER, 1971). Another level, marked by basalt conglomerates and shells (Pectinidae), has been found at 175 m a.s.l. NW of M. Vambolieri. Such deposits, intercalated with the AAC lavas, represent an intermediate Tyrrhenian coastline whereas the M. Vambolieri level (130 m a.s.l.) represents a last Tyrrhenian episode (MONACO *et alii*, 1995).

STRATIGRAPHY

The reconstruction of the eruptive history of the Valverde Center is mostly based on field mapping and stratigraphic interpretation of volcanic products related to this eruptive center. The occurrence of a Tyrrhenian marine conglomeratic horizon and of a paleosol allow us to subdivide the Valverde volcanic succession into three main cycles.

Cycle I

The products of Cycle I consist of lava flows which discontinuously crop out along the southern and eastern foothills of the edifice (Figs. 2 and 3). The lava flows rest upon the Middle Pleistocene sediments and are capped by the Tyrrhenian conglomerates. The lavas are made up of a few flow units, characterized by thicknesses ranging from 1.8 to 4.5 m, showing a massive inner part passing into a poorly to mildly crusted surface. The general facies of the best preserved lava flows is comparable to the P1-P4 and M1-M3 facies of KILBURN & GUEST (1993), suggesting proximal (near vent) and medial regions, respectively. The discontinuity of the outcrops as well as the general facies of the lava flows suggest that they may be related to fissurel eruptions from vents located in the Nizzeti depression.

Cycle II

The products of Cycle II crop out around the Nizzeti depression and are represented by lava flows and pyroclastic products showing dips consistent with a cone-shaped morphology (Fig. 2 and 3).

The early products are made up of brown massive ash deposits which cover the Tyrrhenian conglomerates, the Cycle I products and the Pleistocene sediments. Discontinuous lens of small-size dense clasts (<1 cm), both lithic and juvenile, have been recognized at the base of the ashes, whereas accretionary lapilli are random. The thickness of these deposists ranges from about 4 m in the paleovalleys to 40 cm in the morphological paleohighs (adjacent ridges) (Fig. 3), where they show a rough layering. In the paleovalleys, dark dense scoriae and rounded to angular lithic clasts (lava fragments) are evenly dispersed in the matrix. Preliminary grainsize analyses (on four samples) indicate a very poor sorting ($\sigma\phi$ = 3.2-4.3); Mdϕ values range from 0.8 to 1.7.

The described features of the ash deposits are consistent with a flow mechanism of emplacement. Occurrence of accretionary lapilli and of rounded lithic clasts are also consistent with an origin from ash flows related to phreatomagmatic eruptions. Figure 4a reports the lithic maximum size measured in different stratigraphic sections. Size distribution suggests for these deposits an origin from vents located inside the present-day Nizzeti depression, near Torre Casalotto.

The ash-flow deposits are capped by a thick sequence of lava flows interlayered with scoria fall deposits. The lava flows show thickness and facies similar to that of Cycle I, whereas the fall deposits are made up of dark scoriae, blocks and bombs related to a strombolian activity. The thickness distribution of fall deposits, as derived by measurements carried out along several stratigraphic sections (Fig. 4b), agrees with the vent location inside the Nizzeti depression.

The products of Cycle II are capped by a red brown paleosol, extending more or less continuously in the investigated area and recognizable in all the stratigraphic sections (Fig. 3).

Cycle III

The products of Cycle III lie on the above mentioned paleosol and crop out both inside and outside the Nizzeti depression (Fig. 2). They consist of a uniform pyroclastic sequence related to a single eruption. The products are represented by four normally-graded pumice fall units separated by three levels of thin massive ashes (Fig. 3). In the three lower fall units the pumices are white in colour and the lithic fragments represent about 10%. The fourth fall unit consists of grey pumices with about 20-25% of lithics. The top of the sequence (Fig. 3) consist of a massive ashy to sandy matrix in which grey pumice lapilli, lithics and rare small-size (2-3 mm) coal fragments are scattered. It has been found only inside the Nizzeti depression (Fig. 2), filling paleovalleys. In the proximal sections, the base of this deposit is characterized by a grey pumice level, with usually imbricated fragments. The general features of the top deposits suggest that they represent a non-expanded pyroclastic flow (WILSON, 1980), related to the last eruptive phases of the Valverde Center.

The pumice fall sequence reaches a maximum thickness of 110 cm in the inner sectors of the Nizzeti depression whereas outside, north of Acitrezza and west of Ficarazzi, it is only 10 cm thick (Fig. 4c). The isopach map also shows a dispersion axis elongate in a NNW-SSE direction. The sequence is consistent with a small-size explosive eruption with an emission center located inside the Nizzeti depression. In fact, the areal dispersion of the deposits and the above mentioned imbricated pumices, indicate a flow moving from the inner sectors of the Nizzeti depression towards N and/or NNW. The occurrence of normal grading in the pumice fall beds as well as associated ash-fall levels suggests a magma withdrawal during short-lived, separate, explosive phases (pulsatory behaviour; BURSIK, 1993). The top flow unit may be related to a direct blast, strongly controlled by pre-existing morphology, rather than to the collapse of the eruptive column.

PETROGRAPHY AND GEOCHEMISTRY

Petrographic features

A set of rocks representative of the three cycles has been sampled for petrographic analyses. Lavas of Cycles I and II are characterized by porphyritic textures, with phenocrysts of olivine, clinopyroxene,

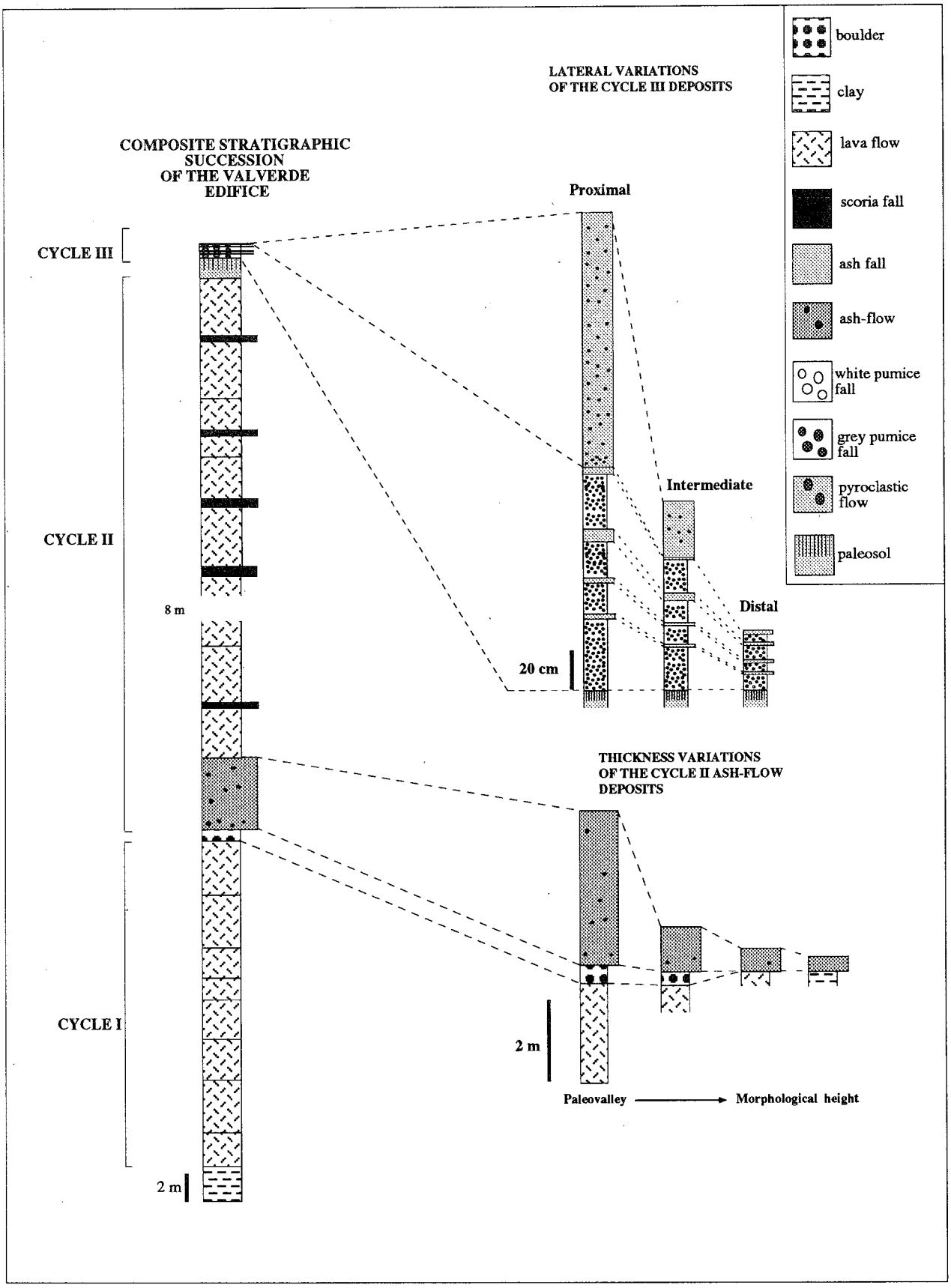

Fig. 3 - Composite stratigraphic section of the Valverde volcanic succession.

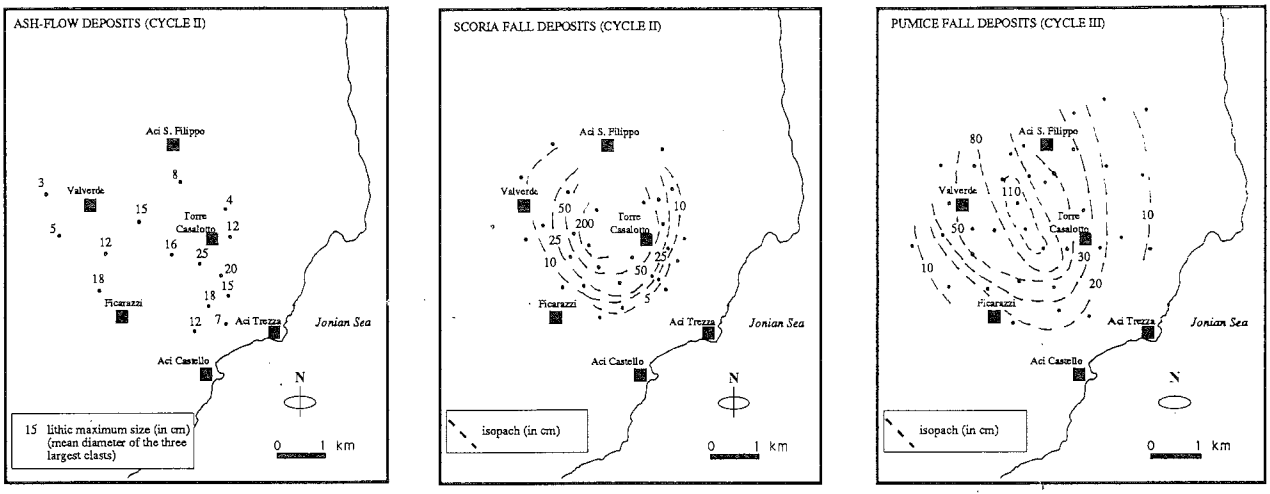

Fig. 4 - A, Maximum size of lithics of ash-flow deposits (Cycle II). B, Isopach map of the upper scoria fall unit of Cycle II. C, Isopach map of the pumice fall deposits of Cycle III.

Table 1 - Selected chemical analyses of the Valverde rocks

Sample	ac3 lava	ac4 lava	ac10 lava	ac12 lava	ac13 lava	ac20 lava	ac21 lava	ac23 lava	ac24 lava	ac1 lava	ac2 lava	ac5 lava	ac6 lava	ac7 lava
Cycle	I	I	I	I	I	I	I	I	I	II	II	II	II	II
SiO_2	50,06	50,88	49,16	48,37	47,83	49,82	49,39	50,32	49,55	50,46	49,54	51,42	49,88	52,38
TiO_2	1,85	1,62	1,55	1,81	1,99	1,85	1,75	1,45	1,47	1,88	1,54	1,56	1,63	1,61
Al_2O_3	19,56	20,25	17,64	18,67	18,12	19,48	19,16	18,73	18,93	19,68	19,94	18,16	18,54	19,25
FeO tot.	9,68	8,62	10,63	10,19	10,93	9,87	10	9,68	9,16	10,04	9,21	11,51	9,32	10,28
MnO	0,15	0,13	0,15	0,15	0,16	0,15	0,15	0,15	0,14	0,15	0,14	0,22	0,15	0,17
MgO	3,66	3,8	7,23	5,67	5,73	3,85	4,69	5,22	6,1	3,56	6,21	3,15	6,13	4,02
CaO	9,34	9,02	9,26	9,25	9,74	9,12	9,6	9,12	8,86	8,94	8,28	8,82	8,91	7,75
Na_2O	4,13	4,14	3,48	3,94	3,77	4,53	4,19	4,07	4,22	4,02	3,18	3,54	3,69	3,19
K_2O	1,05	1,03	0,64	1,23	1,07	1,01	0,84	0,89	1,11	0,82	1,35	0,9	1,27	1
P_2O_5	0,54	0,54	0,4	0,81	0,79	0,4	0,34	0,47	0,59	0,44	0,77	0,74	0,57	0,43
L.O.I.	0,57	0,25	0,15	0,08	0,59	0,04	0,37	-0,07	-0,28	0,94	1,15	2,38	0,02	2,95
Ce	81	85	53	102	102	83	85	74	102	83	123	195	119	136
Ba	530	496	267	537	619	511	444	430	485	558	759	1102	620	711
La	49	44	26	56	61	46	42	42	59	57	75	119	73	84
Ni	24	22	117	43	44	28	34	36	40	31	84	8	70	30
Cr	31	29	185	74	74	31	53	53	67	35	96	17	99	50
V	249	231	243	251	264	250	244	263	225	256	216	183	228	223
Co	31	29	46	37	40	33	35	37	35	36	37	34	37	36
Nb	43	41	23	45	45	46	39	32	46	47	46	95	45	59
Zr	113	102	80	127	112	116	101	95	100	118	126	200	125	160
Y	18	16	16	18	18	18	18	19	16	19	18	26	19	19
Sr	1067	1029	580	981	1389	1030	964	831	964	1050	981	1588	1070	1229
Rb	15	16	9	22	16	18	15	13	18	9	18	22	21	28
Mgv*	43,00	46,79	57,58	52,61	51,12	43,77	48,36	51,85	57,07	41,45	57,36	35,32	56,76	43,83
Zr/TiO_2	0,0061	0,0063	0,0052	0,0070	0,0056	0,0063	0,0058	0,0066	0,0068	0,0063	0,0082	0,0128	0,0077	0,0099
Nb/Y	2,3889	2,5625	1,4375	2,5000	2,5000	2,5556	2,1667	1,6842	2,8750	2,4737	2,5556	3,6538	2,3684	3,1053
La/Ce	0,6049	0,5176	0,4906	0,5490	0,5980	0,5542	0,4941	0,5676	0,5784	0,6867	0,6098	0,6103	0,6134	0,6176
La/Nb	1,1395	1,0732	1,1304	1,2444	1,3556	1,0000	1,0769	1,3125	1,2826	1,2128	1,6304	1,2526	1,6222	1,4237
La/Ba	0,0925	0,0887	0,0974	0,1043	0,0985	0,0900	0,0946	0,0977	0,1216	0,1022	0,0988	0,1080	0,1177	0,1181
P.I.	0,27	0,31	0,49	0,23	0,29	0,34	0,25	0,38	0,21	0,19	0,24	0,36	0,22	0,23
Plagioclase	0,9	0,8	0,6	0,8	1,2	1,1	0,8	0,7	0,8	0,9	1	1,2	1,6	1,2
Femics														

XRF water - free to 100 analyses. MgO and Na_2O by AAS
Mgv* on the basis of Fe_2O_3/FeO = 0,15
P.I. and Plagioclase/Femics ratio by point counting

Ti-magnetite and plagioclase. Clinopyroxene and olivine predominate in the samples of Cycle I, whereas plagioclase usually represents the most abundant phase in the rocks of Cycle II (see Plagioclase/Femics ratio in Table 1). Complex zoning have been usually observed in the plagioclase crystals of both Cycles I and II. Amphibole (kaersutite) and cumulates occur sometimes in the Cycle II lavas. Vesiculated scoria fragments of the strombolian fall deposits show the same mineral association recognized in the interbedded lavas.

The juvenile component of the ash-flow deposits consists of poorly to non vesiculated dark glassy fragments with crystal of plagioclase, clinopyroxene, olivine, Ti-magnetite and kaersutite. Loose glass and crystal fragments are common in the ashy component of the deposits. The rocks of Cycles I and II have P.I. values ranging from 0.21 to 0.49 and from 0.19 to 0.39, respectively (Table 1). Most of the mesostasis are extensively altered by secondary products (hydroxides and clay minerals).

The pumices of Cycle III show a subaphyric texture (P.I. < 0.1). Phenocrysts are represented by plagioclase, clinopyroxene and kaersutite. The mesostasis are characterized by colourless (white pumice) or pale brown (grey pumices) glass fragments. Blended clasts are also present. Rare microphenocrysts of plagioclase occur in the groundmass, whereas zeolites usually occur in the vesicles as products of alteration.

Geochemistry

Relatively fresh samples, representative of the three cycles, have been selected for chemical analyses (Table 1). Cycle III pumices showing a homogeneous glassy matrix have been analyzed whereas blended pumices have been rejected. Because of the occurrence of alteration phenomena in same samples (H20 > 2%, see Table 1), classical classification criteria have been utilized with caution.

TAS (LE MAITRE, 1989), SiO_2 vs Nb/Y and Zr/TiO_2 vs Nb/Y (WINCHESTER & FLOYD, 1977) plots are shown in Figure 5. In the TAS diagram the more evolved rocks of Cycle II fall in the sub-alkaline field.

Continue table 1

Sample	ac8 lava	ac19 lava	ac22 scoria	cm18a grey pumice	cm18b white pumice	cm1a white pumice	cm1b white pumice	cm1c white pumice	cm2 grey pumice	cm3a grey pumice	cm5 white pumice	cm7 white pumice	cm10 grey pumice
Cycle	II	II	II	III	III	III	III	III	III	III	III	III	III
SiO_2	53,7	50,28	48,56	61,63	61,93	61,91	61,75	61,83	61,48	61,34	62,36	62,05	61,62
TiO_2	1,57	1,49	1,3	1,37	1,35	1,37	1,4	1,36	1,44	1,45	1,32	1,43	1,46
Al_2O_3	19,05	18,77	18,14	16,31	16,3	16,35	16,47	16,43	16,47	16,45	16,46	17,04	16,34
FeO tot.	10,25	8,62	9,86	6,31	6,18	6,29	6,49	6,14	6,69	6,61	6,04	6,63	6,69
MnO	0,17	0,14	0,16	0,18	0,18	0,18	0,18	0,18	0,18	0,18	0,18	0,19	0,19
MgO	3,87	5,88	7,24	1,6	1,6	1,62	1,61	1,58	1,72	1,74	1,63	1,58	1,71
CaO	7,21	8,6	10,08	3,36	3,28	3,34	3,35	3,28	3,52	3,58	3,25	3,26	3,54
Na_2O	2,95	4,3	3,49	5,8	5,76	5,43	5,32	5,77	5,17	5,36	5,36	4,72	5,34
K_2O	0,96	1,38	0,82	3,11	3,1	3,16	3,07	3,11	2,95	2,92	3,04	2,76	2,77
P_2O_5	0,36	0,64	0,55	0,36	0,34	0,34	0,35	0,34	0,37	0,38	0,35	0,35	0,36
L.O.I.	3,6	-0,21	-0,17	2,66	2,59	2,78	2,29	2	2,72	2,51	3,08	4,12	2
Ce	142	131	99	242	244	247	244	239	240	244	242	254	238
Ba	728	654	465	1406	1399	1404	1412	1396	1382	1358	1386	1373	1351
La	87	75	56	150	151	152	152	150	149	152	150	153	149
Ni	35	55	50	4	3	3	3	4	3	3	3	5	4
Cr	68	77	114	6	6	7	6	6	6	6	5	8	6
V	215	206	254	80	78	83	79	80	89	90	78	85	89
Co	36	33	39	11	11	12	11	12	13	13	12	14	13
Nb	59	47	38	124	118	120	124	123	118	119	122	116	115
Zr	181	126	76	485	469	464	480	472	452	459	478	461	445
Y	23	16	16	35	34	34	34	34	33	34	34	33	34
Sr	1179	1060	947	795	769	783	789	788	813	827	769	754	879
Rb	32	24	10	73	72	71	73	75	69	68	71	66	65
Mgv*	42,98	57,66	59,44	33,59	34,08	33,94	33,13	33,95	33,92	34,45	34,99	32,24	33,77
Zr/TiO_2	0,0115	0,0085	0,0058	0,0354	0,0347	0,0339	0,0343	0,0347	0,0314	0,0317	0,0362	0,0322	0,0305
Nb/Y	2,5652	2,9375	2,3750	3,5429	3,4706	3,5294	3,6471	3,6176	3,5758	3,5000	3,5882	3,5152	3,3824
La/Ce	0,6127	0,5725	0,5657	0,6198	0,6189	0,6154	0,6230	0,6276	0,6208	0,6230	0,6198	0,6024	0,6261
La/Nb	1,4746	1,5957	1,4737	1,2097	1,2797	1,2667	1,2258	1,2195	1,2627	1,2773	1,2295	1,3190	1,2957
La/Ba	0,1195	0,1147	0,1204	0,1067	0,1079	0,1083	0,1076	0,1074	0,1078	0,1119	0,1082	0,1114	0,1103
P.I.	0,32	0,39	0,26	0,07	0,05	0,06	0,08	0,04	0,08	0,04	0,07	0,06	0,09
Plagioclase / Femics	0,9	1,5	1,3	1,8	1,6	1,6	1,8	2	1,5	1,4	1,8	1,9	2,1

XRF water - free to 100 analyses. MgO and Na_2O by AAS
Mgv* on the basis of $Fe_2O_3/FeO = 0,15$
P.I. and Plagioclase/Femics ratio by point counting

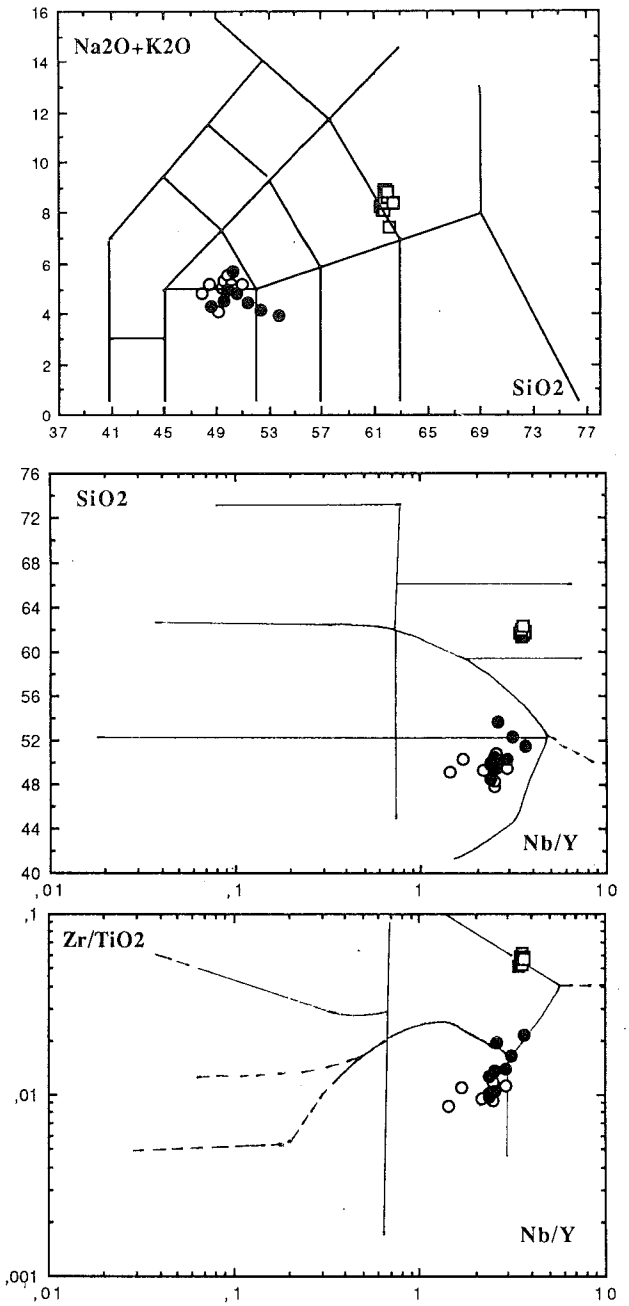

Fig. 5 - TAS (La Maitre, 1989), SiO_2 vs Nb/Y and Zr/TiO_2 vs Nb/Y (Winchester & Floyd, 1977) diagrams from the Valverde rocks. Key: Open circles, Cycle I; dots, Cycle II; squares, Cycle III.

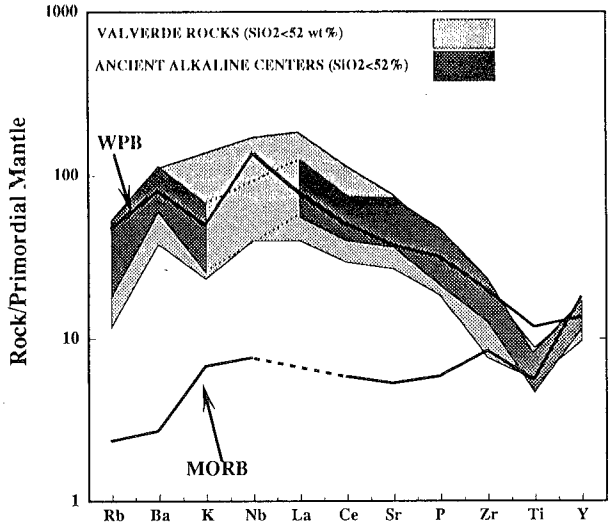

Fig. 6 - Trace element abundances normalized to primordial mantle composition (Wood, 1979) of the Valverde less evolved rocks (SiO_2 > 52 wt %) The average MORB, WPB trends (Pearce, 1982) are reported for comparison as well as the AAC volcanics (data from Cristofolini *et alii*, 1991). The distribution of the Valverde rocks generally mimics that of WPB and AAC.

This may be related to hydration phenomena producing a subtraction of Na_2O and K_2O. In the discrimination diagrams of Winchester & Floyd (1977), the whole set of the Valverde rocks is characterizd by a Nb/Y ratio indicating an alkaline affinity (Nb/Y > 1). In the spider diagram of Figure 6 the Valverde rocks show a pattern consistent with the WPB (Pearce, 1982) as well as with the AAC (Cristofolini *et alii*, 1991). Trace element concentrations in the Valverde rocks are also consistent with the variations observed in the oldest alkaline Etnean products (Joron & Treuil, 1984).

From a compositional point of view, the Valverde rocks are characterized by a bimodal distribution. The rocks of Cycles I and II show SiO_2 contents ranging from 48.37 to 53.7 wt% (basalts, hawaites and mugearites). The pumices of Cycle III are characterized by SiO_2 contents ranging from 61.34 to 62.36 wt% (benmoreites-trachytes). It is interesting to note that evolved products have so far not been recognized in the AAC successions (Cristofolini & Romano, 1982; Joron & Treuil, 1984; Cristofolini *et alii*, 1991). In the general evolution of M.te Etna, trachytic products appear with the formation of the Ellittico caldera (14 ka; Condomines *et alii*, 1982).

The porphyritic character of the Valverde basic rocks suggests that their chemical features do not represent melt compositions. The Mgv* values also indicate small scale fractionation processes during the ascent (Mgv* < 59.44, see Table 1).

In Figure 7 selected major and trace elements vs SiO_2 content are reported. Oxides of Cycles I and II show very similar trends. Samples with constant SiO_2 are characterized by significant variations of TiO_2, Al_2O_3 and P_2O_5, whereas MgO, FeO and CaO abruptly decrease with the SiO_2 increase. With the exception of Cycle III samples, the oxides depict sub-vertical trends. Small variations of TiO_2 and FeO can be also observed in Cycle III rocks. These characters are not related to the different crystal content of the samples but reflect different compositions of the glasses (Table 1).

Trace elements vs SiO_2 content show more complex distributions. Cycle II rocks are enriched in Sr, Ba, Nb, La and Ce in comparison with Cycle I rocks. Generally, these elements show a positive correlation with SiO_2 whereas Ni, Cr and V are characterized by a negative correlation according with their compatible character. Ni and Cr contents of Cycle II rocks range from 8 to 84 ppm and from 17 to 96 ppm, respectively. High Ni and Cr contents have been observed in one lava sample (ac10 in Table 1) of Cycle I. This lava is also characterized by the lowest contents in incompatible elements among all the analyzed lavas.

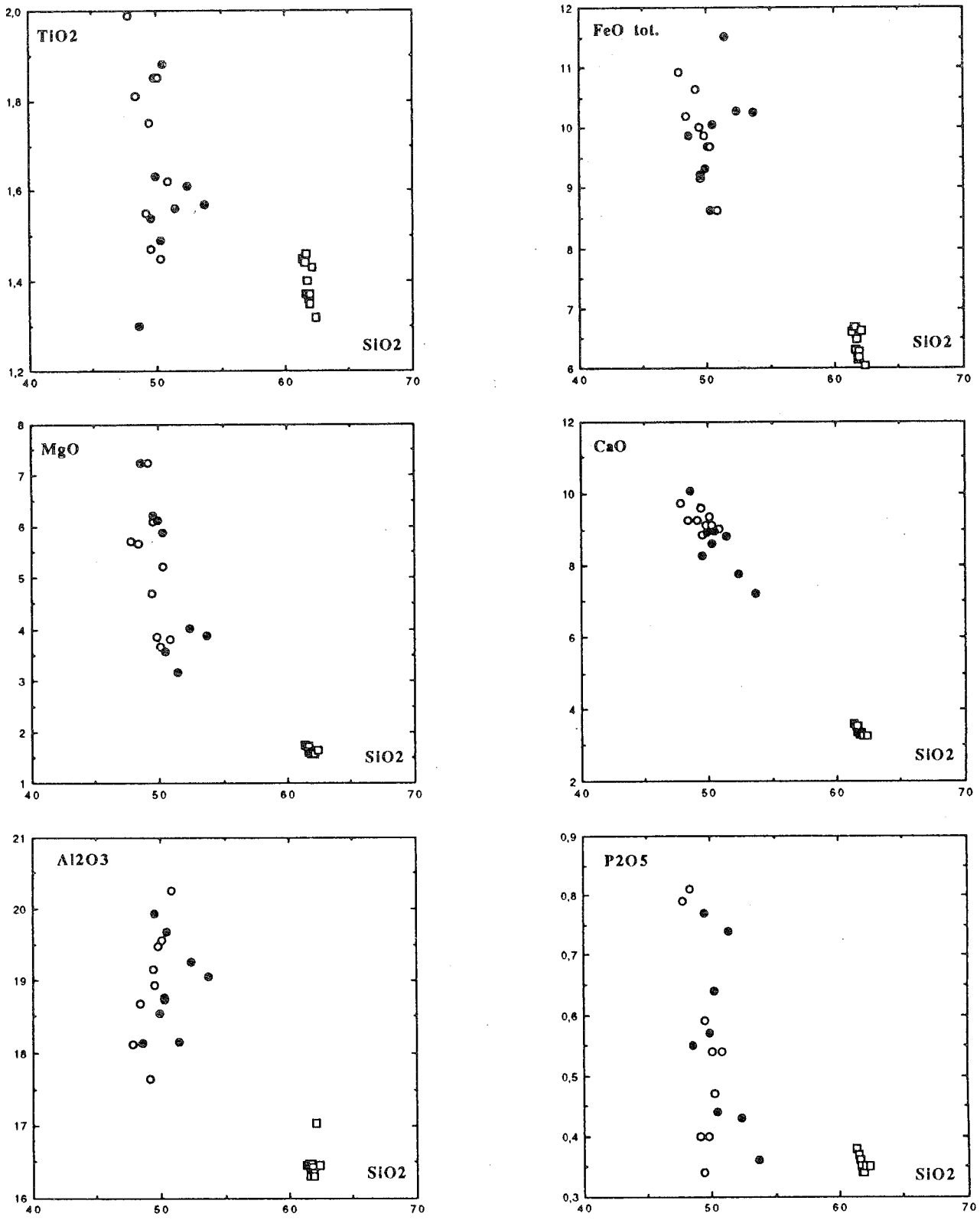

Fig. 7 - SiO_2 vs selected major and trace elements for the studied Valverde samples. Symbols as in Fig. 5.

Taking into account also the low Plagioclase/Femics ratio (0.5) and the high P.I. (0.49) (Table 1), this is the most primitive product sampled from the Valverde Center. The pumices of Cycle III show the highest values of incompatible elements, according with their more evolved character. White pumices are slightly enriched in Zr and Nb and depleted in Sr with respect to the grey pumices.

Trace elements

Selected trace elements vs time for each Cycle are reported in Figure 8. The patterns appear quite consistent with the incompatible or compatible character of the selected elements. Ni and Cr show sub-

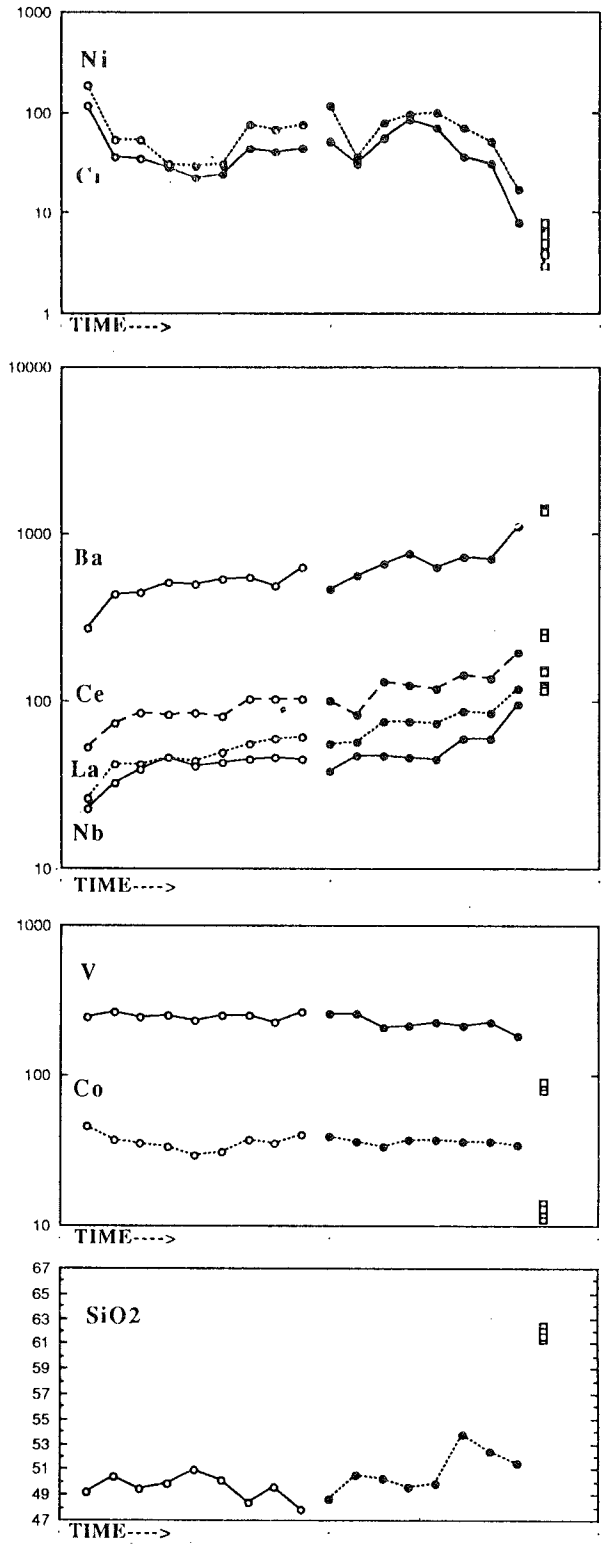

Fig. 8 - Time vs abundances of selected trace elements in the Valverde succession. Symbols as in Fig. 5.

parallel trends as well as La, Ce, Nb and Ba. V and Co also show similar trends. In Cycle I samples, incompatible elements are characterized by a constant increment with time. This trend can be also observed in the rocks of Cycle II but the absolute values of the incompatible elements of the samples at the base of Cycle II are generally lower than the samples at the top of the Cycle I. Ni and Cr are characterized by more complex patterns. Ni and Cr contents decrease abruptly in the lower part of the Cycle I and increase progressively towards the top. In the Cycle II, a first decrease is followed by an increase and then by a strongly depletion towards the top. With the exception of Cycle III rocks, all these trends do not appear related with the SiO_2 (see Fig. 8) and/or crystal content (Table 1).

La/Ce and La/Nb ratios of the three cycles are characterized by significant variations (Fig. 9). In the rocks of Cycle I, La/Ce ratio ranges from 0.491 to 0.605 whereas Cycle II rocks show values ranging from 0.566 to 0.687. The samples of Cycle III are characterized by nearly constant values ($0.602 < La/Ce < 0.628$). Also the La/Ba vs La/Nb-La/Ce diagrams indicate that the ratios between incompatible elements are quite different in Cycles I and II (Fig. 10). In these diagrams, Cycle III samples fall in a intermediate field between the Cycles I and II. No significant differences occur between the La/Ba, La/Nb and La/Ce ratios of the grey and white pumices of Cycle III. It is reasonable to assume that these pumices represent the products of the fractionation from a homogeneous parent magma.

DISCUSSION AND CONCLUSIONS

The main results obtained by the geological and volcanológical study of the Valverde Center can be

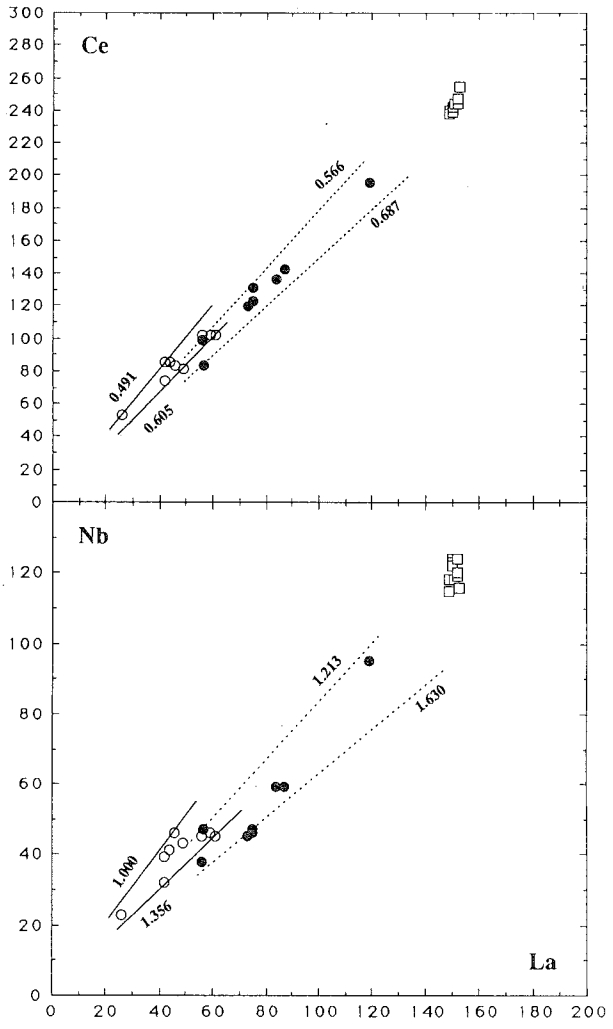

Fig. 9 - La vs Ce and La vs Nb plots for the Valverde rocks. Numbers refer to different ratios between the elements. Symbols as in Fig. 5.

summarized as follows:

a) the early phases of activity of the center have been characterized by basaltic to hawaiitic effusions probably from eruptive fissures located in the eastern and southern sectors of the present-day Nizzeti depression (Cycle I);

b) the products of Cycle II, showing compositions similar to Cycle I, indicate phreatomagmatic, strombolian and effusive activities in a period ranging between 100 and 150 Kyr. In this period, corresponding to the Tyrrhenian sea-level high stand, the Valverde center was built up. The volcanic activity in marine environment may explain the occurrence of the phreatomagmatic deposits at the base of the Cycle II succession;

c) Cycle III products (high-SiO_2 benmoreites and trachytes) are related to a single explosive event producing both fall and flow deposits;

d) during the whole period of activity, the southeastern sector of Mt. Etna underwent a progressive uplifting followed by the collapse of the Valverde center. Therefore, the Nizzeti area represents a morphological depression developed within a general uplifting trend.

Geochemical data also allow one to define the magmatic evolution of the Valverde center. Taking into account the behaviour of the trace elements and the time relationships between the three Cycles, fractional crystallization processes alone cannot explain the whole petrochemical features of the Valverde rocks (Figs. 8, 9 and 10). As La and Ce or Nb are highly incompatible and immobile elements, their ratios are less, or not, affected by mineralogical control and/or other differentiation processes (i.e. gaseous transfer). These elements, whose behaviour is particularly sensitive to the melting processes, may give informations about the evolution of the Valverde rocks.

The La vs La/Ce diagram (Fig. 11) suggests that most of Cycle I lavas (basalts and low-SiO_2 hawaites) represent the result of cooling of liquids generated by different degrees of partial melting of a heterogeneous source (trend **a** in the Fig. 11). Small scale crystallization processes related to slightly different parent magmas can also be reasonable supposed to explain the occurrence of the more evolved products of Cycle I (high-SiO_2 hawaites) (trend **b** in Fig. 11). Cycle II rocks are characterized by sub-parallel horizontal trends (trends **c** and **d** in Fig. 11). It suggests an important role of fractional crystallization processes in the genesis of Cycle II magmas. In this picture, the corresponding parent magma may be considered as a mix between a liquid of Cycle I (point A in Fig. 11) and an end-member liquid of Cycle II (point B). This latter, giving rise to the bottom lavas of Cycle II, may represent a magma derived by a lower degree of partial melting of a source with a La/Ce ratio similar to the point A. Cycle III rocks show petrochemical features consistent with the occurrence of a slightly zoned reservoir. Ratios between incompatible elements (Figs. 9 and 10) indicate that the pumices are the product of fractional crystallization from a parent magma with geochemical features between Cycle I and II (trend **d** in Fig. 11). The occurrence of a paleosol between Cycle II and III rocks also supports this hypothesis. In conclusion, the chemical evolution of the Valverde rocks agrees with the models proposed to explain the petrochemical features of both ancient and recent Etnean lavas (ARMIENTI *et alii*, 1989; CLOCCHIATTI *et alii*, 1992; BARBIERI *et alii*, 1993).

Stratigraphical, volcanological and petrochemical data suggests an evolution of the activity from fissure type to central type, with the formation of a small reservoir in the last eruptive phase (Cycle III). In our opinion, the general evolution of the eruptive center, characterized by the final development of a magmatic reservoir, is strictly related to the tectonic activity. The Valverde area has been affected, since the Middle Pleistocene, by N30°W to N20°E trending normal faults, related to a WNW-ESE extension. The extension has been accommodated by oblique-dextral movements along the NNW-SSE master fault and by dip-slip movements along the NNE-SSW splays (Figs. 1 and 2). The Valverde Center was formed where the NNE-SSW segments branch off from the NNW-SSE oblique master fault, giving rise to a "horse-tail" geometry. In this structural pattern, characterized by oblique extension processes (TRON & BRUN, 1991), volcanism

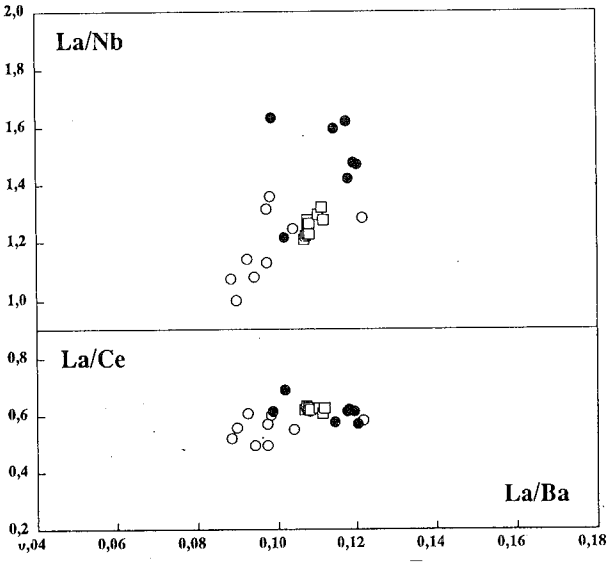

Fig. 10 - La/Ba vs La/Ce and La/Nb for the Valverde rocks. Symbols as in Fig. 5.

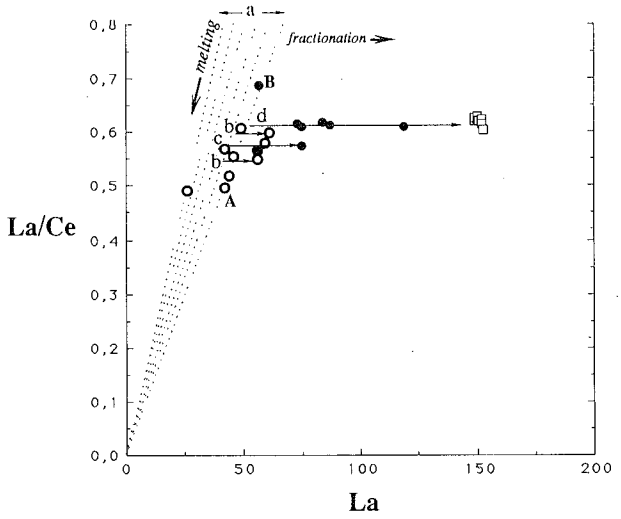

Fig. 11 - La vs La/Ce diagram showing the possible relationships existing between the different Cycles. See text for explanation. Symbols as in Fig. 5.

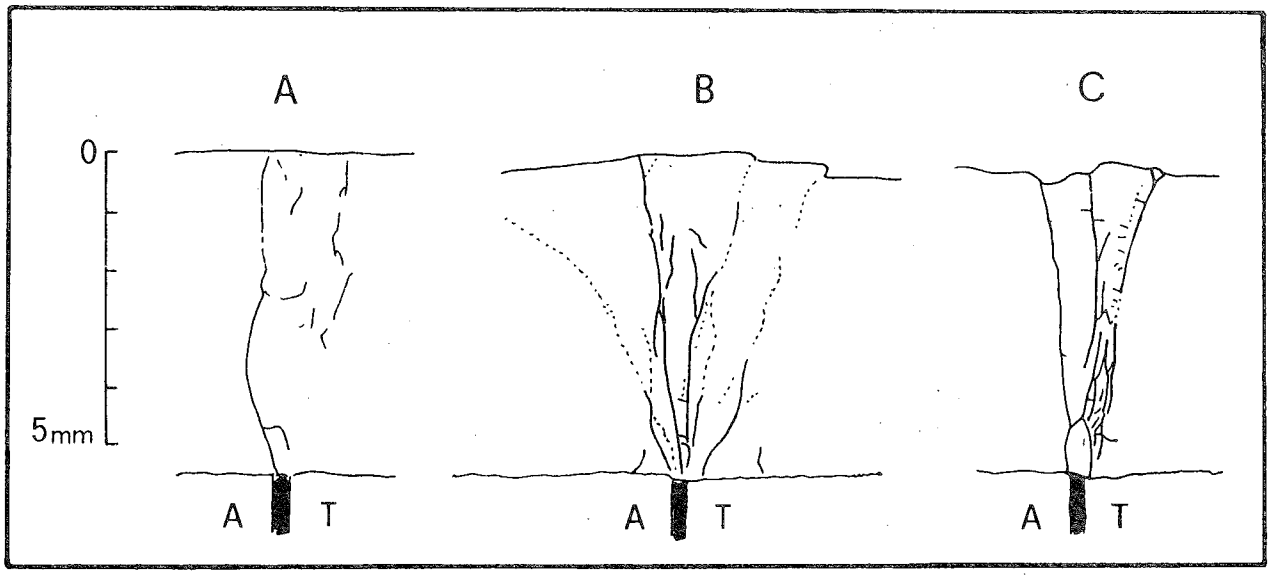

Fig. 12 - Cross-section of a right-lateral shear zone during three different stages of deformation (A, B and C) showing the distinct fracturation patterns. Sense of shear is indicated by T (towards) and A (away). Experimental results from a model on Indiana limestone (by BARTLETT *et alii*, 1981). See text for explanation.

may develop because of the progressive extension and crustal stretching.

A comparison with experimental models on wrench faults (EMMONS, 1969; BARTLETT *et alii*, 1981) shows that the early stages of deformation are characterized by few fractures connecting the basement master fault to the surface (Fig. 12a). As the deformation progresses, new interconnected fractures form at depth (Fig. 12b) whereas, in the final stages, the width of the deformed zone increases with the development of new fractures (Fig. 12c). Similarly, in the Valverde Center, during the early stages of deformation (Fig. 12a) magma could have risen up directly from the mantle to the surface through a basement master fault and a few upper fissures (Cycle I). Successively, the development of interconnecting fractures (Fig. 12b) allowed both mixing and small scale fractionation processes, with the formation of an eruptive center (Cycle II). In the final stages, the occurrence of diffuse fracturing related to progressive faulting (Fig. 12c) favoured the storage of magma at shallow depths. In our opinion, this process allowed the development of small-size magmatic chambers and further fractionation processes (Cycle III).

Experimental models have also shown that along curved segments of wrench faults, subcircular structural depressions may form (EMMONS, 1969). Therefore, the Nizzeti depression could be interpreted as the result of a volcano-tectonic collapse linked to the oblique-extensional framework rather than to the emptying of small-size magmatic chambers.

ACKNOWLEDGEMENTS

We are grateful to G. CELLO, R. MAZZUOLI and L. TORTORICI for stimulating discussions in the field and for carefully revising the manuscript. Many thanks are also due to A.M. DUNCAN and J.E. GUEST for their useful comments and suggestions.

REFERENCES

ARMIENTI P., INNOCENTI F., PETRINI R., POMPILIO M. & VILLARI L. (1989) - *Petrology and Sr-Nd isotope geochemistry of recent lavas from Mt. Etna: bearing on the volcano feeding system.* J. Volcanol. Geotherm. Res., **39**, 315-327.

BARBIERI M., CRISTOFOLINI R., DELITALIA M.C., FORNASERI M., ROMANO R., TADDEUCCI A. & TOLOMEO L. (1993) - *Geochemical and Sr-isotope data on Historic lavas of Mount Etna.* J. Volcanol. Geotherm. Res., **56**, 57-69.

BARTLETT W.L., FRIEDMAN M. & LOGAN J.M. (1981) - *Experimental folding and faulting of rocks under confining pressure.* Tectonophysics, **79**, 255-277.

BOCCALETTI M., GETANEH A. & TORTORICI L. (1992) - *The Main Ethiopian Rift: an example of oblique rifting.* Annales Tectonicae, **6**, 20-25.

BOUSQUET J.C., GRESTA S., LANZAFAME G. & PAQUIN C. (1987) - *Il campo degli sforzi attuali e quaternari nella regione dell'Etna.* Mem. Soc. Geol. It., **38**, 483-506.

BURSIK M. (1993) - *Subplinian eruption mechanisms inferred from volatile and clast dispersal data.* J. Volcanol. Geotherm. Res. 57, 57-70.

CELLO G., CRISCI G.M., MARABINI S., TORTORICI L. (1985) - *Transtensive tectonics in the Strait of Sicily: structural and volcanological evidence from the island of Pantelleria.* Tectonics, **4**(3), 311-322.

CHESTER D.K., DUNCAN A.M., GUEST J.E. & KILBURN C.R.J. (1985) - *Mount Etna; the anatomy of a volcano.* Chapman & Hall, London, 404 pp.

CIVETTA L., CONTICELLI S., D'ANTONIO M., LA VOLPE L., MANETTI P. & POLI G. (1992) - *Mantle domains beneath the Red Sea region: inferences from isotopic and geochemical characteristics of Oligo-Miocene magmatism in Yemen.* Acta Vulcanologica, **2**, 133-145.

CLOCCHIATTI R., WEISZ J., MOSBAH M. & TANGUY J.C. (1992) - *Coexistence de "verres" alcalins et tholéiitiques saturés en CO_2 dans le olivines des hyaloclastites d'Aci Castello (Etna, Sicile, Italie). Arguments en favour d'un manteau anormal et d'un réservoir profond.* Acta Vulcanologica, **2**, 161-173.

CONDOMINES M. & TANGUI J.C. (1976) - *Age de l'Etna determiné par la méthode du déséquilibre radioactif ^{230}Th-^{238}U.* C.R. Acad. Sci. Paris, **282**, 1661-1664.

CONDOMINES M., TANGUI J.C., KIEFFER G. & ALLEGRE C.J. (1982) - *Magmatic evolution of a volcano studied by ^{230}Th-^{238}U disequilibrium and trace elements systematics: the Etna case.* Geochim. Cosmochim. Acta, **46**, 1397-1416.

CRISCI G.M., DE ROSA R., ESPERANZA S., MAZZUOLI R. & SONNINO M. (1991) - *Temporal evolution of a three component system: the island of Lipari (Aeolian Arc, Southern Italy).* Bull. Volcanol., **53**, 207-221.

CRISTOFOLINI R. & ROMANO R. (1982) - *Petrologic Features Of The Etnean Rocks.* Mem. Soc. Geol. It., **23**, 99-115.

CRISTOFOLINI R., CORSARO R.A. & FERLITO C. (1991) - *Variazioni petrochimiche nella successione etnea: un riesame in base a nuovi dati da campioni di superficie e da sondaggi.* Acta Vulcanologica, **1**, 25-37.

EMMONS R.C. (1969) - *Strike-slip rupture patterns in sand models.* Tectonophysics, **7**, 71-87.

IMBO G. (1935) - *I terremoti etnei.* R. Acc. Naz. dei Lincei, **5**, 1-94.

JORON J.L. & TREUIL M. (1984) - *Etude geochimique et petrogenese des laves de l'Etna.* Bull. Volcanol., **46**, 1126-1144.

KIEFFER G. (1971) - *Depôts et niveaux marins et fluviatiles de la région de Catane (Sicile).* Mediterranée, **5-6**, 591-626.

KIEFFER G. (1985) - *Evolution structurale et dynamique d'un grand volcan polygenique: stades d'édification et activité actuelle de l'Etna (Sicile).* Thèse d'Etat Universitè de Clermont-Ferrant, 497 pp.

KIEFFER G. & TANGUY J.C. (1993) - *L'Etna: évolution structurale, magmatique et dynamique d'un volcan "poligénique".* Mém. Soc. Géol. Fr., **163**, 253-271.

KILBURN C.R.J., GUEST J.E. (1993) - *AA lavas of Mt. Etna (Sicily).* In: Active lava flows (edited by C.R.J. KILBURN & G. LUONGO). British Library Cataloguing Biddles LTD, Norfolk (England), pp 73-104.

LE MAITRE R.W. (1989) - *A classification of igneous rocks and glossary of terms. Recomendations of the IUGS Subcommission on the systematics of igneous rocks.* Black-Well, London, 204 pp.

LO GIUDICE E., PATANE G., RASÀ R. & ROMANO R. (1982) - *The structural framework of Mount Etna.* Mem. Soc. Geol. It., **23**, 125-158.

LO GIUDICE E. & RASÀ R. (1986) - *The role of the NNW structural trend in the recent geodynamic evolution of north-eastern Sicily and its volcanic implications in the Etnean area.* J. Geodynamics, **25**, 309-330.

MONACO C. & TORTORICI L. (1995) - *Tettonica estensionale quaternaria nell'Arco Calabro e in Sicilia orientale.* Studi Geol. Camerti, Vol. speciale.

MONACO C. & PETRONIO L. & ROMANELLI M. (1995) - *Tettonica estensionale nel settore orientale del Monte Etna (Sicilia): dati morfotettonici e sismici.* Studi Geol. Camerti, Vol. speciale.

PEARCE J.A. (1982) - *Trace element characteristics of lavas from destructive plate boundaries.* In: Andesites (edited by R.S. THORPE), John Wiley & Sons, Chichester, pp. 525-548.

ROMANO R. (1982) - *Succession of the volcanic activity in the etnean area.* Mem. Soc. Geol. It., **23**, 75-97.

ROMANO R. & STURIALE C. (1981) - *Geologia del versante sud-orientale etneo, F° 270 IV (NO, NE, SO, SE).* Boll. Soc. Geol. It., **100**, 15-40.

TANGUY J.C. (1978) - *Tholeiitic basalt magmatism of Mount Etna and its relations with the alkaline series.* Contr. Min. Petrol., **66**, 51-67.

TRON V. & BRUN J.P. (1991) - *Experiments on oblique rifting in brittle-ductile systems.* Tectonophysics, **188**, 71-84.

WEZEL F.C. (1967) - *I terreni quaternari del substrato dell'Etna.* Atti Acc. Gioienia Sc. Nat. Catania, **6**, 271-282.

WILSON C.J.N. (1980) - *The role of fluidification in the emplacement of pyroclastic flows.* An experimental approach. J. Volcanol. Geotherm. Res., **8**, 231-249.

WINCHESTER J.A. & FLOYD P.A. (1977) - *Geochemical discrimination of different magma series and their differentiation products using immobile elements.* Chemical Geology, **20**, 325-343.

WOOD D.A. (1979) - *A variable veined suboceanic upper mantle. Genetic significance for Mid-Ocean ridge basalts from Geochemical evidence.* Geology, **7**, 499-503.